RSC Advances

PAPER

View Article Online
View Journal | View Issue



Cite this: *RSC Adv.*, 2020, **10**, 14410

# Identification of benzothiazones containing a hexahydropyrrolo[3,4-*c*]pyrrol moiety as antitubercular agents against MDR-MTB†

Xican Ma,‡[ab] Bing Han,‡[ab] Aoyu Wang,[c] Lu Yang,[b] Menghao Huang,[d] Kushan Chowdhury,[d] Jian Gu,*[a] Kai Zhang*[c] and Kai Lv[b]

Received 24th January 2020
Accepted 23rd March 2020

DOI: 10.1039/d0ra00750a

rsc.li/rsc-advances

**IMB1603**, a spiro-benzothiazone compound discovered by our lab, displayed potent anti-MTB activity *in vitro* and *in vivo*. In this study, we reported a series of new BTZs containing the hexahydropyrrolo[3,4-*c*]pyrrol moiety based on the structure of **IMB1603**. Among them, BTZs **11** and **24** displayed potent anti-MTB (MIC < 0.035 μM) and MDR-MTB (MIC, 0.053–0.102 μM) activity, good solubility (1.82–1.85 μg $mL^{-1}$), and low cytotoxicity ($CC_{50}$ > 200 μM), suggesting BTZs **11** and **24** may serve as promising candidates for further study. The molecular docking study of **11** toward DprE was also investigated, and revealed that **11** mimicked the binding pattern of **PBTZ169** in the active site of DprE1.



Tuberculosis (TB) is a chronic infectious disease caused mainly by *Mycobacterium tuberculosis* (MTB).[1] The World Health Organization (WHO) estimated that approximately 10 million people were infected and 1.5 million died from TB worldwide in 2018.[2] The current therapy for TB infected patients requires a combination of four front-line drugs for 6–9 months and does not favor patient compliance. Even worse, the prevalence of multidrug-resistant (MDR) TB and extensively drug-resistant (XDR) TB has exacerbated the situation.[3–5] Although new drugs with novel mechanisms such as bedaquiline, delamanid and pretomanid have been approved in recent years for the treatment of MDR-TB,[6,7] some adverse events or warnings have been noted and limited their use in the clinic.[8] Therefore, there is still an urgent unmet medical need for safer and more effective agents for the treatment of TB.

Benzothiazinones (BTZs), a novel class of TB agents targeting decaprenylphosphoryl-β-D-ribose 2′-epimerase (DprE1),[9,10] exhibited exceptional inhibitory activity against MTB and MDR-MTB strains.[11–13] **PBTZ169** (macozinone) and **BTZ043**, the most advanced BTZ candidates, is currently in phase II[14] and phase I clinical trial[15] for the treatment of both drug-susceptible TB and MDR-TB.[16] BTZ scaffold has become a research hot spot throughout the world for the scientists and researchers working in the field of anti-TB.[17–21]

According to the binding pharmacophore revealed by the crystal structures of **BTZ043**/**PBTZ169** complexed with DprE1, the BTZ core interacted with the active site cavity, whereas the cyclohexane or spirocyclic moiety was located at the protein surface (Fig. 1).[13,16] More precisely, the $CF_3$ group was well placed in a small pocket and interacted with Asn392; the nitro group of **PBTZ169** or **BTZ043** was converted to nitroso which covalently binds to Cys387 or Cys394 residue of DprE1 enzyme, leading to irreversible inactivation of the enzyme.[13,16] It appeared that the BTZ core was crucial for the activity, but the spirocyclic or cyclohexane at the C-2 position might be open for structure modification.

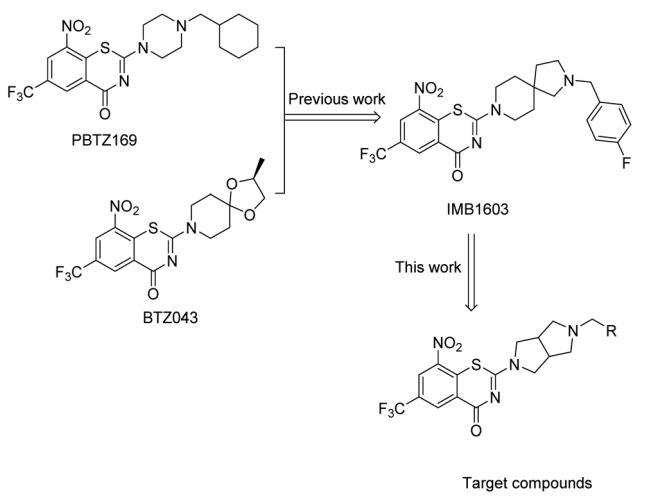


Fig. 1 Design of new BTZs.

[a]*College of Pharmacy, Southwest Minzu University, Chengdu, 610041, China. E-mail: gujiancd@163.com*

[b]*Institute of Medicinal Biotechnology, Chinese Academy of Medical Sciences, Peking Union Medical College, Beijing, 100050, China*

[c]*Department of Pharmaceutical Chemistry, School of Pharmacy, Hebei Medical University, Shijiazhuang, 050017, PR China. E-mail: zhk810728@163.com*

[d]*Department of Biochemistry and Molecular Biology, Indiana University School of Medicine, Indianapolis, IN 46202, USA*

† Electronic supplementary information (ESI) available. See DOI: 10.1039/d0ra00750a

‡ These authors contributed equally to this work.

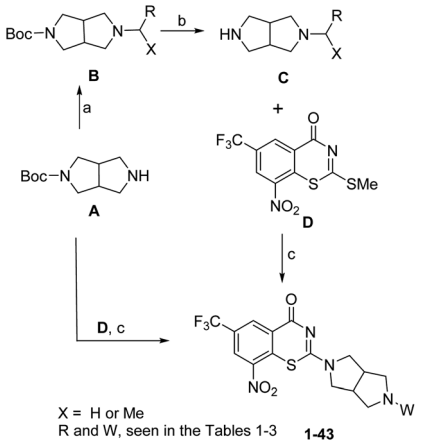


Scheme 1 Reagents and conditions: (a): (i) X = H, ArCHO, $Na(OAc)_3BH$, AcOH, $CH_2Cl_2$, RT, 3–4 h, 71–85%; OR (ii) X = Me, $Ti(OiPr)_4$, acetophenones, MeOH, $NaCNBH_3$, 40 °C, 5–7 h, 30–55%; (b) TFA, DCM, rt, 3–4 h; (c) (i) $Et_3N$, MeOH, 40 °C, 1–1.5 h, 22–41%, two steps; (ii) TFA, DCM, 70% (Boc deprotection in TFA was only needed for compound **36**).

Based on the binding characteristics and reported structure–activity relationship (SAR), our group focused on the discovery of alternative moieties at the C-2 position of BTZ core.[22–25] Recently, we identified **IMB1603** with a spiro-heterocyclic segment as a potent anti-TB lead by combining the structure feature of **PBTZ169** and **BTZ043**.[23] In this study, replacement of the spiro-heterocyclic group of **IMB1603** with hexahydropyrrolo [3,4-*c*]pyrrol gave a new series of BTZs (Fig. 1). The anti-TB activity, solubility, and toxicity of these new BTZs were evaluated, aiming to identify alternative groups at position 2 of BTZs

Table 1 The structure and anti-MTB activity of new BTZs series **1**

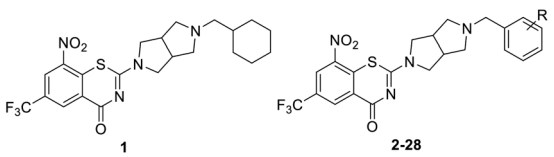


| Compd | R | MIC (μM) | Compd | R | MIC (μM) |
|---|---|---|---|---|---|
| **1** | | 0.462 | **17** | *m*-$NO_2$ | 0.414 |
| **2** | *p*-F | 0.244 | **18** | *m*-$CF_3$ | 0.101 |
| **3** | *p*-Cl | 1.654 | **19** | *m*-MeO | 3.671 |
| **4** | *p*-Br | 0.953 | **20** | *o*-F | 3.595 |
| **5** | *p*-CN | 0.616 | **21** | *p*-F, *m*-F | 0.111 |
| **6** | *p*-$NO_2$ | 0.451 | **22** | *p*-Cl, *m*-Cl | 0.077 |
| **7** | *p*-$CF_3$ | 0.112 | **23** | *p*-F, *m*-Cl | 0.104 |
| **8** | *p*-MeO | 1.832 | **24** | *p*-Cl, *m*-F | <0.035 |
| **9** | *p*-tBu | 0.218 | **25** | *p*-F, *o*-Cl | 0.888 |
| **10** | *p*-Me | 1.926 | **26** | *p*-F, *o*-F | 0.232 |
| **11** | *p*-$CF_3O$ | <0.035 | **27** | *p*-Cl, *o*-Cl | 0.566 |
| **12** | H | 0.796 | **28** | *p*-F, *o*-Br | 0.783 |
| **13** | *m*-F | 0.222 | **PBTZ169** | | <0.035 |
| **14** | *m*-Cl | 0.217 | INH | | 0.262 |
| **15** | *m*-Br | 0.203 | RFP | | 0.166 |
| **16** | *m*-CN | 0.223 | | | |

Table 2 The structure and anti-MTB activity of new BTZs series **2**

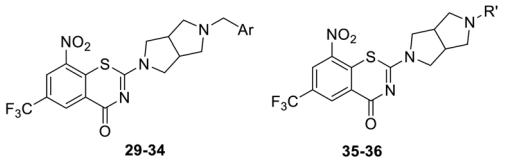


| Compd | Ar or R′ | MIC (μM) |
|---|---|---|
| **12** |  | 0.796 |
| **29** |  | 1.667 |
| **30** |  | 1.849 |
| **31** |  | 1.981 |
| **32** | 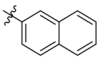 | 0.463 |
| **33** |  | 0.899 |
| **34** | 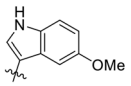 | 27.350 |
| **35** | Boc | 1.720 |
| **36** | H | >40 |
| **PBTZ169** | | <0.035 |

and find optimized potent anti-TB drug candidates with improved drug-like properties through SAR study.

The synthesis of target compounds **1–43** was shown in Scheme 1. Reductive amination of hexahydropyrrolo[3,4-*c*]pyrrol **A** in the presence of aryl aldehydes or acetophenones gave

Table 3 The structure and anti-MTB activity of new BTZs series **3**

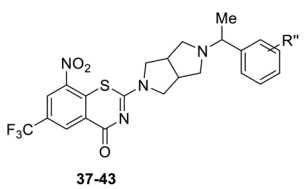


| Compd | R″ | MIC (μM) |
|---|---|---|
| **37** | *p*-$CF_3$ | 0.202 |
| **38** | *p*-$OCF_3$ | 0.209 |
| **39** | *p*-F, *m*-F | 0.110 |
| **40** | *p*-Cl, *m*-F | 0.219 |
| **41** | *p*-F, *m*-Cl | 0.108 |
| **42** | *m*-F, *m*-F | 0.205 |
| **43** | *p*-F, *m*-F, *m*-F | 0.189 |
| **PBTZ169** | | <0.035 |

Table 4 Anti-MDR-MTB activity and cytotoxicity of selected compounds

| | MIC (μM) | | | |
|---|---|---|---|---|
| Compd | MDR-MTB1[a] | MDR-MTB2[a] | $CC_{50}$[b] (μM) | Water solubility[c] (mg $mL^{-1}$) |
| **7** | 0.080 | 0.053 | 166.37 | 2.30 |
| **11** | 0.085 | 0.053 | >200 | 1.85 |
| **18** | 0.209 | 0.112 | 55.77 | 2.29 |
| **21** | 0.119 | 0.058 | 38.63 | 3.50 |
| **22** | 0.110 | 0.056 | 27.31 | 1.94 |
| **23** | 0.115 | 0.058 | 40.79 | 2.01 |
| **24** | 0.102 | 0.073 | >200 | 1.82 |
| **39** | 0.121 | 0.087 | 54.98 | 2.97 |
| **41** | 0.188 | 0.097 | 50.68 | 2.55 |
| **PBTZ169** | <0.035 | <0.035 | >200 | 0.90[d] |
| INH | >40 | >40 | ND | NT |
| RFP | >40 | >40 | ND | NT |

[a] MDR-MTB1 (MDR-MTB 16833) and MDR-MTB2 (MDR-MTB 16995) were obtained from the State Laboratory of Tuberculosis Reference of China. [b] The 50% cytotoxic concentration. [c] The water solubility was tested in 0.01 M HCl solution (approximate pH 2.0). [d] This data was from ref. 24.

compound **B**. Thereafter, deprotection of the Boc group in trifluoroacetic (TFA) gave the intermediate **C**. Coupling of BTZ core **D** with **A** or **C** in the presence of $Et_3N$ (TEA) afforded the target compounds **1–35** and **37–43**. Removing the Boc group of **35** in TFA gave the target compound **36**.

The target compounds **1–43** were initially screened for *in vitro* activity against MTB H37Rv ATCC 27294 strain using the Microplate Alamar Blue Assay (MABA).[26] The minimum inhibitory concentration (MIC) was defined as the lowest concentration effecting a reduction in fluorescence of >90% relative to the mean of replicate bacterium-only controls. The MIC values of the compounds along with isoniazid (INH), rifampicin (RFP) and **PBTZ169** were presented in Tables 1–3 for comparison.

As shown in Table 1, BTZs **1** and **2** with cyclohexyl and *p*-fluorobenzyl group from **PBTZ169** and **IMB1603** were initially synthesized and evaluated. The MIC value of BTZ **2** was lower than that of **1**, and comparable to that of INH. According to our previous SAR findings of spiro-BTZs, the substituents at the phenyl ring were crucial for anti-TB activity.[23] In parallel with the spiro-BTZ series, we synthesized compounds **3–28** with diversity R substituents at the phenyl ring. To our delight, compounds **7**, **11**, **18** and **21–24** displayed increased potency (MIC < 0.15 μM). Especially, compound **11** with *p*-$CF_3O$ and **24** with *p*-Cl, *m*-F were found to exhibit comparable anti-TB activity to **PBTZ169** (MIC < 0.035 μM). It is interesting that moving the *para* substituent to *meta* position led to an improved anti-TB activity (**2–7** *vs.* **13–19**), while transferring to the *ortho* position seemed to result in a decreased potency (**2** *vs.* **20**). Notably, BTZs with double substituents at the *para* and *meta* position of the benzyl moiety showed better anti-TB activity (MIC < 0.15 μM) than the corresponding mono-substituted BTZs (**21–24** *vs.* **2–3** and **13–14**), whereas introducing double substituents to the *para* and *ortho* position of benzyls were not well tolerated (**25–28**, MIC > 0.2 μM).

As a continuing SAR study, BTZs **29–34** with other aromatic cyclic groups as replacement of the benzyl moiety were explored. Compared to BTZ **12**, the pyridyl analogues **29–31** and β-naphthalene **33** showed decreased potency, whereas the α-naphthalene **32** displayed a slightly increased anti-TB activity. The indole moiety was also not favored, leading to a dramatically decreased anti-TB activity (**34**, MIC = 27.35 μM). In addition, BTZ **35** with Boc-group was synthesized and proved to display moderate anti-TB potency (MIC < 2 μM). Removal of the R′ group, as in compound **36**, led to a total loss of anti-TB potency (MIC > 40 μM), indicating the existence of N–H bond might not be tolerated at the C2-position of the BTZ core.

Finally, as shown in Table 3, BTZs with a methyl group at the linker were investigated in this set. The R″ group of **37–41** were selected from the BTZs with potent anti-TB activity in Table 1 (MIC < 0.15 μM). Compared to the corresponding BTZs in Table 1, the introduction of a methyl group resulted in a decreased anti-TB potency (**37–41** *vs.* **7**, **11**, **21**, **23–24**). In addition, BTZs **42** with double *m*-F and **43** with *p*-F, double *m*-F, were designed and synthesized according above SAR findings. However, the anti-TB potency of BTZs **42–43** was also not as good as we expected, both of them displayed lower anti-TB activity than **39**.

On the bases of above studies, BTZs **7**, **11**, **18**, **21–24**, **39**, and **41** with potent anti-TB activity (MIC < 0.15 μM) were evaluated against two clinical isolated MDR-MTB (16833 and 16995) strains resistant to both INH and RFP.§ As shown in Table 4, although the MIC values of these new BTZs were all lower than that of **PBTZ169** (MIC < 0.035 μM), most of them displayed considerable anti-MDR-TB activity (MIC < 0.15 μM).

These compounds were then tested for mammalian cell cytotoxicity using Vero cells¶ measured as a concentration

§ The *M. tuberculosis* strains used in these studies included the laboratory strain H37Rv (ATCC 27294; American Type Culture Collection, Rockville, MD) and drug-resistant clinical isolates. All isolates were obtained from the State Laboratory of Tuberculosis Reference of China.

¶ African green monkey kidney (Vero) cells were purchased from the American Type Culture Collection (ATCC), and were cultured in Minimum Essential Medium (MEM) supplemented with 10% fetal bovine serum (FBS) (GBICO) and antibiotics (100 U per mL penicillin and 100 mg per mL streptomycin) at 37 °C in a 5% $CO_2$ incubator.

 

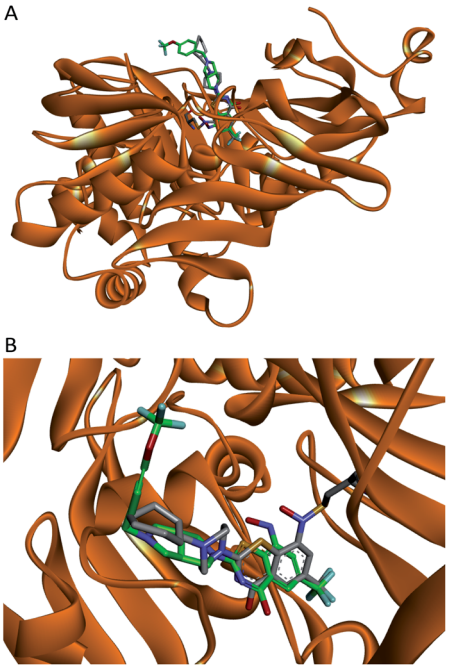


Fig. 2 Overlay of the docking hydroxylamine intermediate of **11** (carbons are green) on the crystallized semimercaptal adduct (carbons are off white). (A) The overall view of the binding pattern; (B) close-up view of the DprE1 active site.

inhibiting 50% growth ($CC_{50}$) as compared to a no-treatment control and the results were reported in Table 4. Most of the tested targets displayed higher cytotoxicity than that of **PBTZ169**. However, to our delight, compounds **11** and **24** showed low cytotoxicity ($CC_{50}$ > 200 μM). Subsequently, considering acidic gastrointestinal environments, these new BTZs were evaluated for their water solubility at pH 2 (0.01 M HCl solution) by using an HPLC-UV method.[23] All of them displayed good solubility (1.82–3.50 μg $mL^{-1}$), and were more water-soluble than **PBTZ169** (0.90 μg $mL^{-1}$).

It was reported that BTZs bound to the DprE1 dimer–dimer interface,[13,16] indicating that the new BTZs might also bind the same site. Thus, we predicted the binding mode of compound **11** in the DprE1 dimer–dimer interface (PDB code: 4NCR) through molecular docking using CDDOCK module of Discovery Studio 3.5. Since the intrinsic ligand **PBTZ169** was crystallized as a covalent adduct with DprE1, it was necessary to optimize the docking protocol of **11** into DprE1. Briefly, the benzothiazinone ligand (semimercaptal) present in the crystal structure was deleted and no hydrogen was added to the formed thiolate of Cys 387. The reduced hydroxylamine form of **11** was docked in the same binding pocket forming the semimercaptal adduct as reported before.[17] The docking study revealed that **11** mimicked the binding pattern of **PBTZ169** in the active site of DprE1 (Fig. 2B). The (trifluoromethoxy)benzyl moiety of **11** was placed outside the pocket and showed high flexibility as the cyclohexylmethyl moiety of **PBTZ169**, whereas the BTZ core occupied the inner part of the cavity (Fig. 2A).

## Conclusions

In summary, a series of new BTZs containing hexahydropyrrolo [3,4-*c*]pyrrol moiety were designed and synthesized based on the spiro-BTZ **IMB1603** discovered in our lab. Many of them exhibited potent *in vitro* anti-TB activity. Especially, compounds **11** and **24** were found to display excellent anti-MTB activity against the drug-sensitive MTB strain H37Rv (MIC < 0.035 μM), and also potent anti-MDR-MTB activity against the two drug-resistant clinical isolates (MIC, 0.053–0.102 μM). In addition, BTZs **11** and **24** showed low cytotoxicity ($CC_{50}$ > 200 μM), and exhibited better water solubility than **PBTZ169**, suggesting both of them may serve as new and promising candidates for further antitubercular drug discovery. The molecular docking results suggested that **11** mimicked the binding pattern of **PBTZ169** in the active site of DprE1. Studies to determine the PK profiles and *in vivo* efficacy of **11** and **24** are currently under way.

## Conflicts of interest

There are no conflicts to declare.

## Acknowledgements

This work is supported by the National Mega-project for Innovative Drugs (2018ZX09721001-004-007; 2018ZX09711001-007-002), National Natural Science Foundation of China (81872753).

## References

1 C. L. Daley, *Thorac. Surg. Clin.*, 2019, **29**, 19–25.
2 World Health Organization, *Global Tuberculosis Report*, 2019, www.who.int/tb/publications/global_report/en/.
3 M. AlMatar, H. AlMandeal, I. Var, B. Kayar and F. Koksal, *Biomed. Pharmacother.*, 2017, **91**, 546–558.
4 J. Herrmann, J. Rybniker and R. Muller, *Curr. Opin. Biotechnol.*, 2017, **48**, 94–101.
5 S. Tiberi, N. du Plessis, G. Walzl, M. J. Vjecha, M. Rao, F. Ntoumi, S. Mfinanga, N. Kapata, P. Mwaba, T. D. McHugh, G. Ippolito, G. B. Migliori, M. J. Maeurer and A. Zumla, *Lancet Infect. Dis.*, 2018, **18**, e183–e198.
6 D. T. Hoagland, J. Liu, R. B. Lee and R. E. Lee, *Adv. Drug Delivery Rev.*, 2016, **102**, 55–72.
7 N. J. Ryan and J. H. Lo, *Drugs*, 2014, **74**, 1041–1045.
8 Side Effects of bedaquiline and pretomanid, https://www.drugs.com/sfx/pretomanid-side-effects.html, https://www.drugs.com/sfx/bedaquiline-side-effects.html.
9 M. Brecik, I. Centarova, R. Mukherjee, G. S. Kolly, S. Huszar, A. Bobovska, E. Kilacskova, V. Mokosova, Z. Svetlikova, M. Sarkan, J. Neres, J. Kordulakova, S. T. Cole and K. Mikusova, *ACS Chem. Biol.*, 2015, **10**, 1631–1636.
10 R. V. Chikhale, M. A. Barmade, P. R. Murumkar and M. R. Yadav, *J. Med. Chem.*, 2018, **61**, 8563–8593.
11 V. Makarov, G. Manina, K. Mikusova, U. Mollmann, O. Ryabova, B. Saint-Joanis, N. Dhar, M. R. Pasca, S. Buroni, A. P. Lucarelli, A. Milano, E. De Rossi, M. Belanova, A. Bobovska, P. Dianiskova, J. Kordulakova,

C. Sala, E. Fullam, P. Schneider, J. D. McKinney, P. Brodin, T. Christophe, S. Waddell, P. Butcher, J. Albrethsen, I. Rosenkrands, R. Brosch, V. Nandi, S. Bharath, S. Gaonkar, R. K. Shandil, V. Balasubramanian, T. Balganesh, S. Tyagi, J. Grosset, G. Riccardi and S. T. Cole, *Science*, 2009, **324**, 801–804.

12 V. Makarov, S. T. Cole and K. Johnsson, *J. Am. Chem. Soc.*, 2010, **132**, 13663–13665.

13 J. Neres, F. Pojer, E. Molteni, L. R. Chiarelli, N. Dhar, S. Boy-Rottger, S. Buroni, E. Fullam, G. Degiacomi, A. P. Lucarelli, R. J. Read, G. Zanoni, D. E. Edmondson, E. De Rossi, M. R. Pasca, J. D. McKinney, P. J. Dyson, G. Riccardi, A. Mattevi, S. T. Cole and C. Binda, *Sci. Transl. Med.*, 2012, **4**, 150ra121.

14 Phase 2a study of **PBTZ169**, https://clinicaltrials.gov/ct2/show/NCT03334734.

15 Phase 1 study of **BTZ043**, https://clinicaltrials.gov/ct2/show/NCT04044001.

16 V. Makarov, B. Lechartier, M. Zhang, J. Neres, A. M. van der Sar, S. A. Raadsen, R. C. Hartkoorn, O. B. Ryabova, A. Vocat, L. A. Decosterd, N. Widmer, T. Buclin, W. Bitter, K. Andries, F. Pojer, P. J. Dyson and S. T. Cole, *EMBO Mol. Med.*, 2014, **6**, 372–383.

17 R. Tiwari, P. A. Miller, L. R. Chiarelli, G. Mori, M. Sarkan, I. Centarova, S. H. Cho, K. Mikusova, S. G. Franzblau, A. G. Oliver and M. J. Miller, *ACS Med. Chem. Lett.*, 2016, **7**, 266–270.

18 L. Xiong, C. Gao, Y. J. Shi, X. Tao, J. Rong, K. L. Liu, C. T. Peng, N. Y. Wang, Q. Lei, Y. W. Zhang, L. T. Yu and Y. Q. Wei, *RSC Adv.*, 2018, **8**, 11163–11176.

19 P. Li, B. Wang, X. Zhang, S. M. Batt, G. S. Besra, T. Zhang, C. Ma, D. Zhang, Z. Lin, G. Li, H. Huang and Y. Lu, *Eur. J. Med. Chem.*, 2018, **160**, 157–170.

20 R. Tiwari, P. A. Miller, S. Cho, S. G. Franzblau and M. J. Miller, *ACS Med. Chem. Lett.*, 2015, **6**, 128–133.

21 T. Karoli, B. Becker, J. Zuegg, U. Mollmann, S. Ramu, J. X. Huang and M. A. Cooper, *J. Med. Chem.*, 2012, **55**, 7940–7944.

22 R. Zhang, K. Lv, B. Wang, L. Li, B. Wang, M. Liu, H. Guo, A. Wang and Y. Lu, *RSC Adv.*, 2017, **7**, 1480–1483.

23 K. Lv, X. You, B. Wang, Z. Wei, Y. Chai, B. Wang, A. Wang, G. Huang, M. Liu and Y. Lu, *ACS Med. Chem. Lett.*, 2017, **8**, 636–641.

24 K. Lv, Z. Tao, Q. Liu, L. Yang, B. Wang, S. Wu, A. Wang, M. Huang, M. Liu and Y. Lu, *Eur. J. Med. Chem.*, 2018, **151**, 1–8.

25 A. Wang, K. Lv, Z. Tao, J. Gu, L. Fu, M. Liu, B. Wan, S. G. Franzblau, C. Ma, X. Ma, B. Han, A. Wang, S. Xu and Y. Lu, *Eur. J. Med. Chem.*, 2019, **181**, 111595.

26 C. Trefzer, M. Rengifo-Gonzalez, M. J. Hinner, P. Schneider, V. Y. Lu, M. Zheng, B. Wang, L. Fu, W. Zhao, P. Li, J. Xu, H. Zhu, H. Jin, D. Yin, H. Huang, A. M. Upton and Z. Ma, *Antimicrob. Agents Chemother.*, 2011, **55**, 5185–5193.

 